Chinese Journal of Aeronautics, 2013,26(4): 935–942

Chinese Society of Aeronautics and Astronautics
& Beihang University

Chinese Journal of Aeronautics

cja@buaa.edu.cn
www.sciencedirect.com

In-plane corrugated cosine honeycomb for 1D morphing skin and its application on variable camber wing

Liu Weidong [a], Zhu Hua [a,*], Zhou Shengqiang [a], Bai Yalei [a], Wang Yuan [b], Zhao Chunsheng [a]

[a] *State Key Laboratory of Mechanics and Control of Mechanical Structures, Nanjing University of Aeronautics and Astronautics, Nanjing 210016, China*
[b] *Institute of Science, PLA University of Science and Technology, Nanjing 211101, China*

Received 24 April 2012; revised 11 June 2012; accepted 17 August 2012
Available online 28 April 2013

KEYWORDS

Cosine honeycomb;
Flexible skin;
Mechanical properties;
Morphing wing;
Smart structure

Abstract A novel 0-Poisson's ratio cosine honeycomb support structure of flexible skin is proposed. Mechanical model of the structure is analyzed with the energy method, finite element method (FEM) and experiments have been performed to validate the theoretical model. The in-plane characteristics of the cosine honeycomb are compared with accordion honeycomb through analytical models and experiments. Finally, the application of the cosine honeycomb on a variable camber wing is studied. Studies show that mechanical model agrees well with results of FEM and experiments. The transverse non-dimensional elastic modulus of the cosine honeycomb increases (decreases) when the wavelength or the wall width increases (decreases), or when the amplitude decreases (increases). Compared with accordion honeycomb, the transverse non-dimensional elastic modulus of the cosine honeycomb is smaller, which means the driving force is smaller and the power consumption is less during deformation. In addition, the cosine honeycomb can satisfy the deforming requirements of the variable camber wing.

1. Introduction

Morphing aircraft is drawing considerable attention all over the world for its capability of self-adaption during various flight conditions.[1,2] The researches on morphing aircraft mainly concentrate on morphing wing for it allows a single aircraft to perform multiple missions effectively and efficiently.[3–7] As described by Thill et al.,[8] a morphing skin can be envisaged as an aerodynamic fairing to cover an underlying morphing structure and transfer aerodynamic loads of the morphing wing, so flexible skin becomes one of the key technologies of morphing aircraft.[9] Thill et al.[8] pointed out three main areas of research in the review of morphing skin technology: compliant structures, shape memory polymers (SMP), and elastomeric skins. Hetrick et al.[10] proposed compliant structures based on a tailored internal structure and a traditional skin material to allow small amount of trailing edge camber change. These resin-matrix-composite skins are unsuitable because they are not lightweight and unable to achieve large strains

* Corresponding author. Tel.: +86 25 84896131.
E-mail addresses: 314116796@qq.com (W. Liu), hzhu103@nuaa.edu.cn (H. Zhu).

Peer review under responsibility of Editorial Committee of CJA.

1000-9361 © 2013 Production and hosting by Elsevier Ltd. on behalf of CSAA & BUAA. Open access under CC BY-NC-ND license.
http://dx.doi.org/10.1016/j.cja.2013.04.015

when needed. Perkins et al.[11] and Bye and McClure[12] studied the flexible skin based on the material of SMP. SMP skin can get large deformation when heated and cooling and can return to its initial state by re-heating and re-cooling. However, the skin is also not light and manufacturing of the skin is complicated; and besides, it is difficult to implement heating of the SMP to reach transition temperature in the wind tunnel test and it is a high-risk option. Flanagan et al.[13] have been successfully implemented the elastomeric skin on the MFX-1 UAV. The elastomer skin is reinforced by ribbons stretched taught immediately underneath the skin, which proved suitable for wind tunnel testing. However, suitable improvements over the skin, such as a better developed substructure, can be more efficient for morphing. Yokozeki et al.[14] proposed a corrugated flexible skin structure. Refs.[15–17] further studied the equivalent models of several corrugated panels. The structure forms of out-of-plane corrugations and was manufactured from carbon fiber plain woven fabrics. Low transverse non-dimensional elastic modulus (the ratio of transverse equivalent stiffness modulus to the elastic modulus of raw material, E_x/E) can be obtained by choosing appropriate parameters of the structure. However, the thickness in the normal direction of the structure has to be large enough so as to get a low transverse non-dimensional elastic modulus and thus the structure is not light enough for application. Moreover, the fabrication of the structure is complicated. Olympio and Gandhi[18,19] studied 0-Poisson's ratio honeycombed structures, the hybrid and accordion honeycomb. The two honeycombs, whose transverse non-dimensional elastic moduli have nothing to do with the thicknesses in the normal direction, are lighter than structures mentioned above. There into accordion honeycomb is lighter than hybrid honeycomb. In addition, these two flexible honeycombs can be easily manufactured by water jet cutting. Gandhi and Anusonti-Inthra[20] brought into focus some design considerations for flexible skins. It is significant that the skins must have low in-plane stiffness to minimize actuation energy. Traditional flexible honeycombs such as hybrid and accordion honeycomb mentioned above can be further improved to raise the efficiency of the deformation. So structure with lower transverse non-dimensional elastic modulus should be developed to constitute a more efficiency flexible skin.

Taking the advantages of the corrugated structure and the honeycombs mentioned above, a new kind of in-plane corrugated cellular structure, cosine honeycomb is proposed to satisfy the requirements of the flexible skin. Similar to accordion honeycomb, the in-plane corrugated honeycomb is lighter and has better manufacturability than other traditional flexible structures. Most significant of all, it has a lower transverse non-dimensional elastic modulus than the existing flexible honeycombs and is more conducive to morphing. First, mechanical properties are studied and verified by finite element method (FEM) and experiments. Then comparison analyses and verification experiments on cosine and accordion honeycombs have been done to see the differences of the transverse non-dimensional elastic moduli and the energies required by morphing between the two structures. Finally the application of the cosine honeycomb on the flexible skin is discussed.

2. Mechanical properties

The cosine honeycomb mentioned above consists of two supports (one is on the left side of the whole structure and the other is on the right), cosine beams and longitudinal beams, as shown in Fig. 1 (in which F is the tension load, and U the displacement load). The structure is designed for flexible skin and should change its shape when needed. Here the in-plane characteristics of the structure are studied through mechanics method, FEM and experiments.

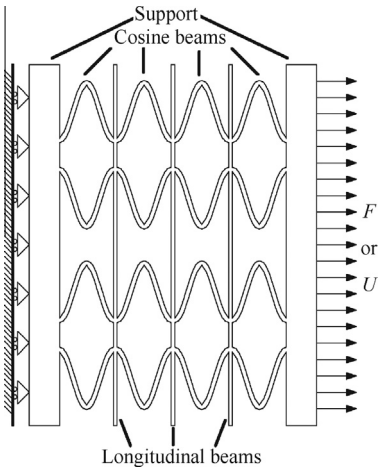

Fig. 1 Structure of cosine honeycomb.

2.1. Transverse properties

This type of cosine honeycomb is basically to deform in one dimension, so tension-compression characteristics of the honeycomb structure are the main objectives to study. Hence the left support of the structure is clamped; the other support is loaded with pulling or pushing pressure or displacement load, as shown in Fig. 1. Then the transverse non-dimensional elastic modulus of the structure could be measured by the corresponding deformation or counter-force.

The deformation of the longitudinal beams is far smaller than the cosine beams and the longitudinal beams have little influence on the transverse non-dimensional elastic modulus of the structure in the load case when the structure is loaded in the transverse direction. The basic cosine cell is picked out to study. Suppose the amplitude of the cosine beam is h, half-wavelength is l, width is t, and normal thickness is b, as shown in Fig. 2.

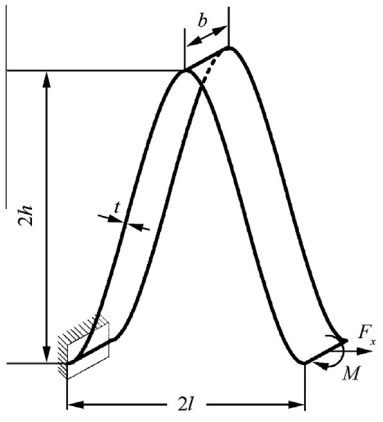

Fig. 2 Single cosine beam.

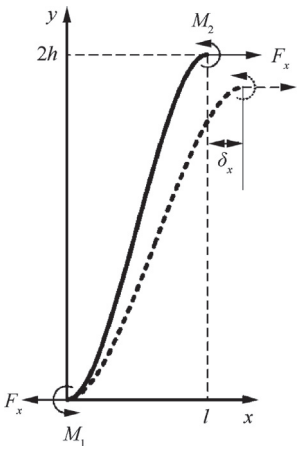

(a) Half-wavelength

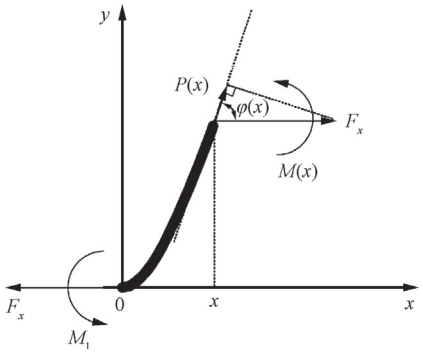

(b) 0-x segment of half-wavelength

Fig. 3 Force analysis.

The construction of the cosine honeycomb and the load case are symmetrical, so half-wavelength structure is taken to do the force analysis, as shown in Fig. 3(a). The tension and moment on the left side are assumed to be F_x and M_1. The tension on the right side is also F_x due to equilibrium condition. The moment on the right side is assumed to be M_2.

The equation of the half-wavelength structure is

$$y = h\left(1 - \cos\frac{\pi}{l}x\right) \quad x = [0, l] \tag{1}$$

Take 0–x segment of the half-wavelength structure for study, as shown in Fig. 3(b). As mentioned above, the force and moment on the left side are still F_x and M_1; the force on the right side is F_x; the moment on the right side is different here, and is assumed to be $M(x)$. Due to equilibrium condition, it can be obtained that

$$M(x) = F_x h\left(1 - \cos\frac{\pi}{l}x\right) - M_1 \tag{2}$$

Angle of rotation of the right end face is

$$\theta(x) = \int_0^x \frac{M(x)}{EI}\mathrm{d}x + C \tag{3}$$

where E is the elastic modulus of raw material, I the moment of inertia, and C a constant.

Boundary conditions of angle of rotation are

$$\begin{cases} \theta(0) = 0 \\ \theta(l) = 0 \end{cases} \tag{4}$$

From Eqs. (1)–(4) it can be figured out that

$$M(x) = -F_x h\ \cos\frac{\pi}{l}x \tag{5}$$

Taking the shaft force into consideration, the shaft force at x is the component of the tension F_x

$$P(x) = F_x \cos\ \varphi(x) \tag{6}$$

where $\cos\varphi(x) = 1/\sqrt{1 + (\mathrm{d}y/\mathrm{d}x)^2}$..

The shear force has little impact on the transverse non-dimensional elastic modulus and so it is neglected. Based on virtual force principle, it can be described that

$$\delta_x = \int \frac{M_F M_{F1}}{EI}\mathrm{d}s + \int \frac{P_F P_{F1}}{Ef}\mathrm{d}s \tag{7}$$

where δ_x is the horizontal displacement of the right end of the half-wavelength structure, f the cross sectional area, M_F and M_{F1} are the internal bending moments under the actual load and unit load conditions, P_F and P_{F1} the internal tensile forces under the actual load and unit load conditions, $\mathrm{d}s = \sqrt{1 + (\mathrm{d}y/\mathrm{d}x)^2}\mathrm{d}x$.

From the basic definitions of mechanics, that is

$$\sigma_x = \frac{F_x}{(2h + t)b} \tag{8}$$

$$\varepsilon_x = \frac{\delta_x}{l} \tag{9}$$

the transverse non-dimensional elastic modulus is

$$\frac{E_x}{E} = \frac{\pi^3 t^3}{2(2h + t)}\left[\left(4l^2 + 4\pi^2 h^2 + \pi^2 t^2\right)A + \left(4\pi^2 h^2 - 4l^2\right)B\right]^{-1} \tag{10}$$

where $A = EK\left(\pi\sqrt{-h^2}/l\right)$, $B = EE\left(\pi\sqrt{-h^2}/l\right)$, $EK(\cdot)$ is the first kind of completely elliptic integral function, and $EE(\cdot)$ the second one.

In addition, it can be easily predicted by theoretical analysis that the deformation along y direction of the longitudinal beams is almost zero when the whole structure is loaded in x direction, so the transverse Poisson's ratio $v_{xy} \approx 0$.

2.2. Longitudinal properties

The longitudinal beams bear the load while the cosine beams do not, when it is applied to the structure in longitudinal direction. Suppose the width of the longitudinal beams is t_w, and the force applied to them in longitudinal direction is F_y, as shown in Fig. 4. The equivalent stress is

$$\sigma_y = \frac{F_y}{2(t_w + l)b} \tag{11}$$

The equivalent strain is

$$\varepsilon_y = \frac{F_y}{2Ebt_w} \tag{12}$$

The longitudinal non-dimensional elastic modulus is

$$\frac{E_y}{E} = \frac{\sigma_y}{\varepsilon_y E} = \frac{t_w}{t_w + l} \tag{13}$$

Analogous to transverse load case, the deformation along transverse direction of the cosine beams is almost zero when the whole structure is loaded in y direction, so the longitudinal Poisson's ratio $v_{yx} \approx 0$.

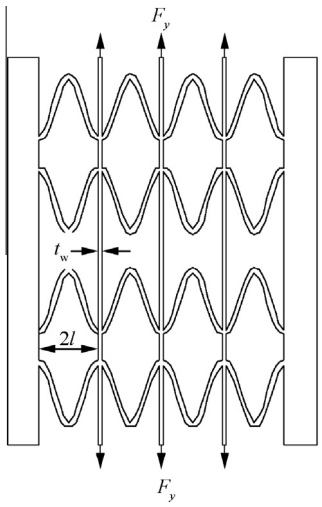

Fig. 4 Load in longitudinal direction.

2.3. FEM verification

The longitudinal properties are concise and explicit, so the transverse non-dimensional elastic modulus is to be verified primarily. Half-wavelength structure is to be studied as above. Half-wavelength l, amplitude h, width t were set as parameters and parametric model was set up by ANSYS parametric design language (APDL), as shown in Fig. 5.

The left side is clamped while the right side is applied with a displacement load U_x, then the counter-force can be obtained and the transverse non-dimensional elastic modulus can be calculated. The model is meshed with solid45 elements. The elastic modulus is set to be 1.7 GPa, considering the material adopted in the experiments. The Poisson's ratio is set to be 0.3. Changing the values of l, h and t, the transverse non-dimensional elastic moduli can be calculated.

2.4. Experimental verification

Cosine honeycombs with different parameters are manufactured from polyoxymethylene (POM) by milling machine. POM, which has favorable physical, mechanical and chemical characteristics, is a kind of resin. Its elastic modulus is 1.7 GPa and Poisson's ratio is 0.3. The width of the two supports on either hand is designed to be large to reduce the local effect when the structure is loaded on the boundaries. One of the samples is shown in Fig. 6.

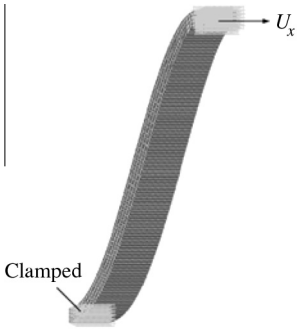

Fig. 5 FEM model.

The samples are tested on the computer controlled electronic universal test machine. The experimental apparatus is shown in Fig. 7. Both sides of the sample are fixed to the clamps by adapting pieces. The displacement between the two supports and the corresponding tension are collected by the computer when the tension is applied to the structure. Then the non-dimensional elastic modulus can be figured out.

2.5. Results analysis of analytical model, FEM and experiments

Figs. 8–10 show the transverse non-dimensional elastic modulus of cosine honeycomb versus half-wavelength, amplitude and width respectively.

As shown in the Figs. 8–10, the results of analytical model, FEM and experiments generally consist with each other. Nonetheless, the experiments results are somehow different from the analytical model. The differences between the analytical model and experiments results are mainly caused by manufacture. For the milling cutter is not thin enough, the fillets at the corners of the structure increase the stiffness of the samples. From the figures it is clear that the transverse non-dimensional elastic modulus of the cosine honeycomb increases (decreases) when the half-wavelength or the width increases (decreases). On the contrary, when the amplitude increases (decreases), the modulus decreases (increases). Fig. 8 shows that

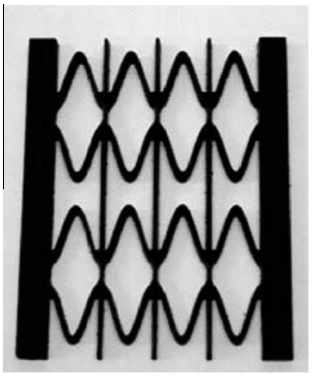

Fig. 6 Sample of cosine honeycomb.

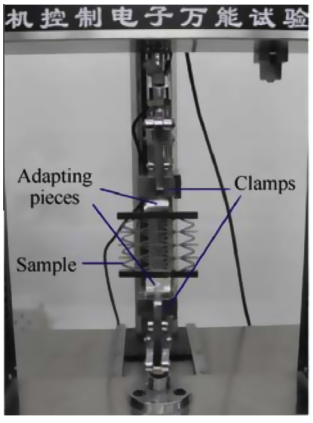

Fig. 7 Test of non-dimensional elastic modulus of cosine honeycomb.

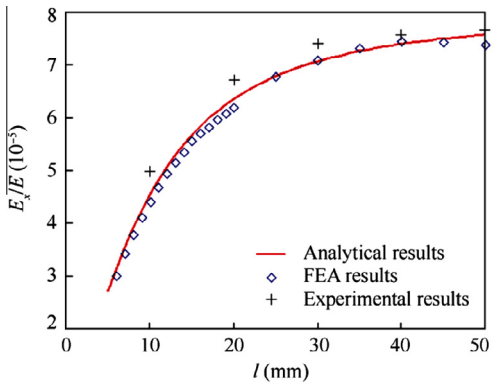

Fig. 8 E_x/E vs l (h = 10 mm, t = 1 mm).

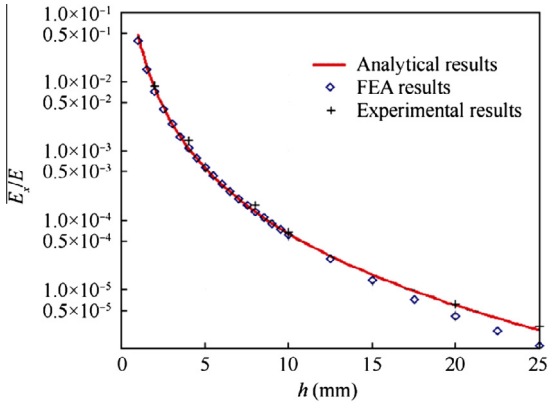

Fig. 9 E_x/E vs h (l = 20 mm, t = 1 mm).

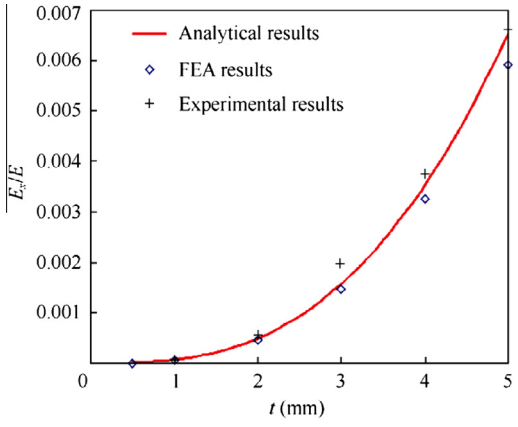

Fig. 10 E_x/E vs t (l = 20 mm, h = 10 mm).

the transverse non-dimensional elastic modulus grows quickly when the half-wavelength is small. With the growth of half-wavelength, the rate of growth of modulus slows down. It can be seen from the curves in Figs. 9 and 10 that the variation of modulus is close to exponential manner with the amplitude and width.

3. Comparison between cosine and accordion honeycombs

As mentioned above, many researchers have proposed kinds of structures for flexible skin. It is necessary to figure out the comparative advantage of cosine honeycomb with the existing structures. Accordion honeycomb is comparatively splendid structure and is selected to make a comparison.

3.1. Comparison between analytical models

Bubert[21] has studied the transverse properties of accordion honeycomb. The transverse non-dimensional elastic modulus of accordion honeycomb is given as

$$\frac{E_{ax}}{E} = \frac{lt^3}{8h^3\sqrt{l^2+4h^2}} \tag{14}$$

Figs. 11–13 are the moduli of the cosine honeycomb and accordion honeycomb versus certain parameters. The transverse non-dimensional elastic modulus of accordion honeycomb varies with parameters more obviously than cosine honeycomb. It should be noticed that the transverse non-dimensional elastic modulus of cosine honeycomb is always lower than accordion honeycomb with the same parameters.

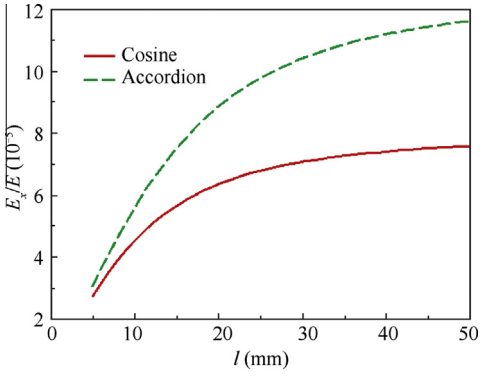

Fig. 11 E_x/E vs l (h = 10 mm, t = 1 mm).

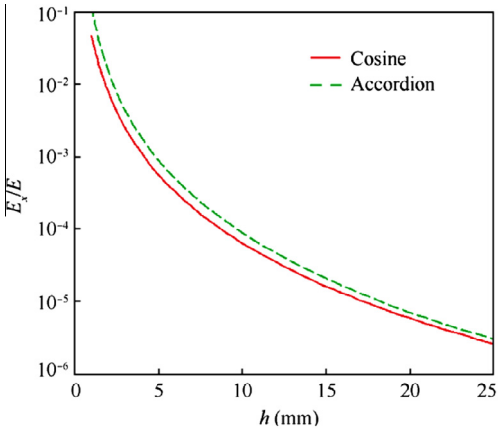

Fig. 12 E_x/E vs h (l = 20 mm, t = 1 mm).

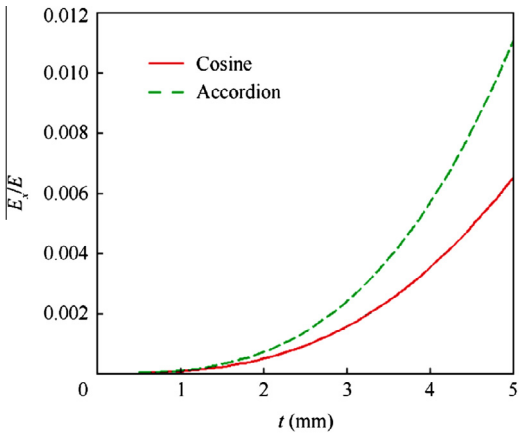

Fig. 13 E_x/E vs t (l = 20 mm, h = 10 mm).

3.2. Experimental comparison

Samples of the two structures are manufactured with the same parameters as shown in Table 1.

The material for the samples and test machine are the same as mentioned in Section 2.4. Fig. 14 shows the comparison experiment of two different structures. Gandhi and Anusonti-Inthra[20] indicate that strain capability of about 2% would be more than adequate for airfoil camber applications. Here a global strain of 3%, that is 4.8 mm (total transverse length of cosine beams is 160 mm), is to be achieved by stretching.

As shown in Fig. 15, the accordion honeycomb requires a tension of 4.62 N and the strain energy is 11.088×10^{-3} J while the cosine honeycomb needs a tension of 2.56 N and the strain energy is 6.144×10^{-3} J when achieves the global strain of 3%. It is clear that the driving force required by transverse deformation of the latter has a reduction of about 44.6% compared with the former, and so is the driving power. When it is applied to the flexible skin, it can reduce the burden of deformation actuators.

Table 1 Parameters of two samples.

Parameter	l (mm)	h (mm)	t (mm)	t_w (mm)
Value	20	10	1	1

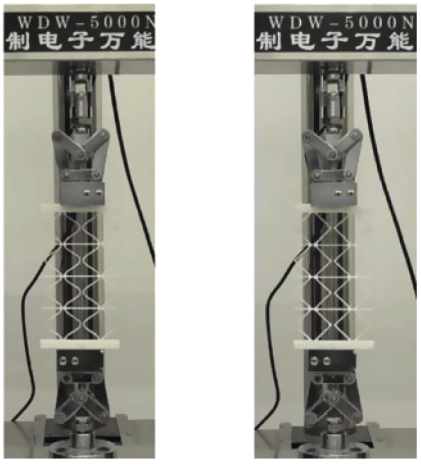

(a) Cosine honeycomb (b) Accordion honeycomb

Fig. 14 Comparison test.

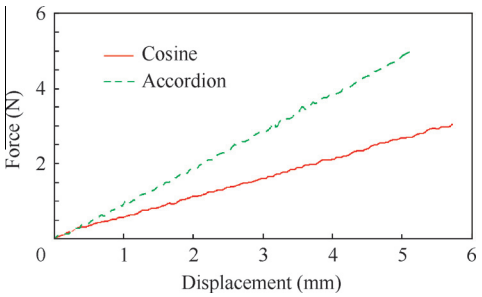

Fig. 15 Results of comparison test.

4. Application of cosine honeycomb

Spillman[22] pointed out that the use of variable gapless wing camber can reduce drag, mass and costs for a transport aircraft. Bartley-Cho et al.[23] developed a kind of adaptive trailing edge for smart wing. Yin[24] studied the stiffness requirement of flexible skin for variable trailing-edge camber wing. A kind of variable camber wing is developed based on the previous researches. The chordwise length of deformation section of the skin is 63.819 mm. A deformation of 2.43 mm could be sufficient due to calculation when the trailing edge has a downward deflection of 10°. So the transverse strain of the skin structure is 3.8%. Considering the assembly of the elastic structure, the whole transverse length is finally set to be 80 mm. The deformation part is 63 mm, so the width of each support is 8.5 mm, as shown in Fig. 16.

Considering the physical dimension of the structure, the wavelength, amplitude of the cosine beams and the width of longitudinal beams are determined first to make the transverse elastic modulus of structure as small as possible. Then, the

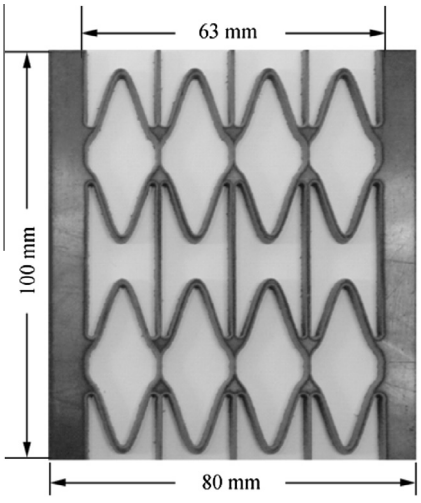

Fig. 16 Skin structure used for variable camber wing.

Table 2 Parameters of the structure.

Parameter	l (mm)	h (mm)	t (mm)	t_w (mm)
Value	7.5	8	1.2	1

width of the cosine beams is chosen and verified by FEM to make sure that the structure can achieve the global strain of 3.8%. The main parameters are set as Table 2. POM is used to manufacture this structure. The results of the FEM and experiment indicate that the transverse stiffness of the cosine honeycomb is only 0.187 MPa, and is just 1.1×10^{-4} of the raw material's stiffness. A distributed force of 27.6 N/m is required to apply to the right edge of the structure to obtain the strain of 3.8%.

FEM result shows that the cosine honeycomb with the parameters shown in Table 2 obtains a maximum local strain of 0.28% while undergoing 3.8% compression globally, a 13.5:1 ratio. For material elastic limit strains of the order of 1%–2% (typical of common polymer engineering materials such as POM as mentioned by Tweedie and van Vliet[25]), the allowed maximum global strains of the structure would be 13.5%–27%. The required strain of 3.8% is below the allowed maximum global strain and therefore allows analysis based upon the assumption that the material is linearly elastic. So the structure will fully recover and return to its original shape when unloaded.

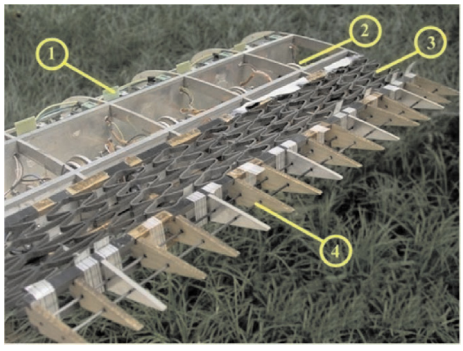

Note: 1—Driving governor; 2—Ultrasonic motor; 3—Cosine type inner support of skin; 4—Trailing edge.

Fig. 17 Inner structures of variable camber wing.

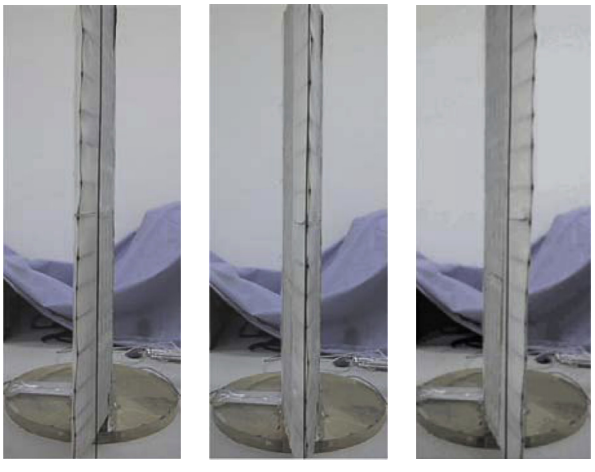

(a) Downward deflection (b) Undeformed (c) Upward deflection

Fig. 18 Undeformed and deformed variable camber wing.

The inner structures including cosine honeycomb of the variable camber wing are shown in Fig. 17. The structures are assembled at the 60%–80% section of the chord length and covered with sheets of silicone elastomer, forming the upper and lower surfaces of the morphing part of wing. The skin is glued to the honeycomb with a pre-tension to avoid wrinkling when the structure is under compression. Experiments show that the cosine honeycomb can be neatly driven by the actuators and meet the deformation requirements. The model of variable camber wing has the ability to change the camber upwards and downwards, as shown in Fig. 18.

5. Conclusions

A kind of in-plane corrugated cosine honeycomb structure for flexible skin is proposed. In-plane mechanical properties of cosine honeycomb are studied. Transverse non-dimensional elastic modulus is obtained by virtual force principle, a kind of energy method and is verified through FEM and experiments. Comparison analyses show that cosine honeycomb is softer in transverse direction than the existing structures for flexible skin. Besides, it is lightweight and has good manufacturability, so it is more suitable for morphing. The application of cosine honeycomb on variable camber wing is studied. It works well for the wing. Actually, this kind of structure is designed for one-dimensional morphing wing. So besides variable camber wing, it is also suitable for the telescope wing.

Acknowledgements

This study was co-supported by National Natural Science Foundation of China (Nos. 50905085, 91116020) and National Science Foundation for Post-doctoral Scientists of China (No. 2012M511263).

References

1. Sofla AYN, Meguid SA, Tan KT, Yeo WK. Shape morphing of aircraft wing: status and challenges. *Mater Des* 2010;**31**(3):1284–92.
2. Barbarino S, Bilgen O, Ajaj RM, Friswell MI, Inman DJ. A review of morphing aircraft. *J Intell Mater Syst Struct* 2011;**22**(9):823–77.
3. Icardi U, Ferrero L. Preliminary study of an adaptive wing with shape memory alloy torsion actuators. *Mater Des* 2009;**30**(10):4200–10.
4. Diaconu CG, Weaver PM, Mattioni F. Concepts for morphing airfoil sections using bi-stable laminated composite structures. *Thin Wall Struct* 2008;**46**(6):689–701.
5. Wu J, Lu YP. A distributed coordinated control scheme for morphing wings with sampled communication. *Chin J Aeronaut* 2010;**23**(3):364–9.
6. Djavareshkian MH, Esmaeli A, Parsani A. Aerodynamics of smart flap under ground effect. *Aerosp Sci Technol* 2011;**15**(8):642–52.
7. Bettini P, Airoldi A, Sala G, di Landro L, Ruzzene M, Spadoni A. Composite chiral structures for morphing airfoils: numerical analyses and development of a manufacturing process. *Compos B* 2010;**41**(2):133–47.

8. Thill C, Etches J, Bond I, Potter K, Weaver P. Morphing skins. *Aeronaut J* 2008;**112**(1129):117–39.
9. Zhang P, Zhou L, Qiu T. A new flexible honeycomb structure and its application in structure design of morphing aircraft. *Acta Aeronaut Astronaut Sin* 2011;**32**(1):156–63 Chinese.
10. Hetrick JA, Osborn RF, Kota S, Flick PM, Paul DB. Flight testing of mission adaptive compliant wing. Report No.: AIAA-2007-1709; 2007.
11. Perkins DA, Reed JL, Havens E. Morphing wing structures for loitering air vehicles. Report No.: AIAA-2004-1888; 2004.
12. Bye DR, McClure PD. Design of a morphing vehicle. Report No.: AIAA-2007-1728; 2007.
13. Flanagan J, Strutzenberg R, Myers R, Rodrian J. Development and flight testing of a morphing aircraft, the NextGen MFX-1. Report No.: AIAA-2007-1707; 2007.
14. Yokozeki T, Takeda SI, Ogasawara T, Takashi I. Mechanical properties of corrugated composites for candidate materials of flexible wing structures. *Compos A Appl Sci Manuf* 2006;**37**(10):1578–86.
15. Xia Y, Friswell MI, Saavedra Flores EI. Equivalent models of corrugated panels. *Int J Solids Struct* 2012;**49**(13):1453–62.
16. Kress G, Winkler M. Corrugated laminate homogenization model. *Compos Struct* 2010;**92**(3):795–810.
17. Kress G, Winkler M. Corrugated laminate analysis: a generalized plane strain problem. *Compos Struct* 2011;**93**(5):1493–504.
18. Olympio KR, Gandhi F. Flexible skins for morphing aircraft using cellular honeycomb cores. *J Intell Mater Syst Struct* 2010;**21**(17):1719–35.
19. Olympio KR, Gandhi F. Zero Poisson's ratio cellular honeycombs for flex skins undergoing one-dimensional morphing. *J Intell Mater Syst Struct* 2010;**21**(17):1737–53.
20. Gandhi F, Anusonti-Inthra P. Skin design studies for variable camber morphing airfoils. *Smart Mater Struct* 2008;**17**(1):015025–33.
21. Bubert EA, Woods BKS, Keejoo L, Curt KS, Wereley NM. Design and fabrication of a passive 1D morphing aircraft skin. *J Intell Mater Syst Struct* 2010;**21**(17):1699–717.
22. Spillman JJ. The use of variable camber to reduce drag, weight and costs of transport aircraft. *Aeronaut J* 1992;**96**(951):1–9.
23. Bartley-Cho JD, Wang DP, Martin CA, Kudva JN, West MN. Development of high-rate, adaptive trailing edge control surface for the smart wing Phase 2 wind tunnel model. *J Intell Mater Syst Struct* 2004;**15**(4):279–91.
24. Yin WL. Stiffness requirement of flexible skin for variable trailing-edge camber wing. *Sci China Technol Sci* 2010;**53**(4):1077–81.
25. Tweedie CA, van Vliet KJ. Contact creep compliance of viscoelastic materials via nanoindentation. *J Mater Res* 2006;**21**(6):1576–89.

Liu Weidong received the B.S. degree in aircraft design and engineering from Nanjing University of Aeronautics and Astronautics in 2008 and became a Ph.D. student from then on. His main research interests are mechanical design and theory, morphing aircraft design and so on.

Zhu Hua is an associate professor at College of Aerospace Engineering, Nanjing University of Aeronautics and Astronautics. He received the Ph.D. degree from the same university in 2007. His current research interests are mechanical electronic engineering and piezoelectric actuators.